

Reaction of $\text{Rh}_2(\text{OOCCH}_3)_4$ with Acetamide: Crystal and Molecular Structure of $[\text{Rh}_2(\text{HNOCCH}_3)_4 \cdot 2\text{H}_2\text{O}] \cdot 3\text{H}_2\text{O}$

M. Q. Ahsan, I. Bernal,* and J. L. Bear*

Received May 13, 1985

The reaction of $\text{Rh}_2(\text{OOCCH}_3)_4$ with excess molten acetamide was found to occur via a stepwise exchange of bound acetate by acetamide anions generated in situ. The products were separated by liquid chromatography. Mass spectral data obtained from the isolated fractions show that $\text{Rh}_2(\text{OOCCH}_3)_3(\text{HNOCCH}_3)$, three geometric isomers of $\text{Rh}_2(\text{OOCCH}_3)_2(\text{HNOCCH}_3)_2$, one isomer of $\text{Rh}_2(\text{OOCCH}_3)(\text{HNOCCH}_3)_3$, and one isomer of $\text{Rh}_2(\text{HNOCCH}_3)_4$ were the only products obtainable from the reaction. The three geometric isomers of $\text{Rh}_2(\text{OOCCH}_3)_2(\text{HNOCCH}_3)_2$ could only be separated on an analytical scale and, therefore, have not been collected in sufficient amounts for structural characterization. Crystals of compound 1, $[\text{Rh}_2(\text{HNOCCH}_3)_4 \cdot 2\text{H}_2\text{O}] \cdot 3\text{H}_2\text{O}$, were obtained from water. Compound 1 crystallizes in the space group $C2/c$, with cell constants of $a = 11.466$ (1) Å, $b = 12.290$ (3) Å, $c = 14.812$ (4) Å, $\beta = 96.83$ (1)°, and $V = 2072.42$ Å³. A total of 3233 data were used in the solution and refinement of the structure, which converged to $R = 2.58\%$ and $R_w = 2.86\%$. The tetraamidate derivative consists of a pair of Rh (II) ions (Rh-Rh = 2.415 (1) Å) bridged by four acetamide ions arranged such that each Rh has a pair of N donors in a cis arrangement. The Rh-N distances (average 2.008 Å) are distinctly shorter than the Rh-O distances (average 2.073 Å), and the Rh-O(H₂O) bond is 2.352 (2) Å. All hydrogen atoms were found and individually refined to positions producing accepted values of the E-H bonds (E = C or N), thus differentiating N from O in the acetamide ligand. The Rh 3d_{5/2} binding energy of all the acetamide substitution products were determined by photoelectron spectroscopy. The Rh 3d_{5/2} binding energy decreases by ~0.2 eV with the addition of each successive acetamide bridging ligand, resulting in a binding energy for $\text{Rh}_2(\text{HNOCCH}_3)_4$ of 308.0 eV. The radical cation $\text{Rh}_2(\text{HNOCCH}_3)_4^+$ has almost the same Rh 3d_{5/2} binding energy as $\text{Rh}_2(\text{OOCCH}_3)_4$, which shows that the exchange of the four acetate bridges by four acetamide ions is equivalent, in terms of metal-centered electron density, to adding one electron to $\text{Rh}_2(\text{OOCCH}_3)_4$.

Introduction

Until recently, studies of the effect of changing bridging ligands on dinuclear Rh(II)-Rh(II) were, by and large, confined to ligands containing oxygen donors.¹ For these substances, equatorial plane ligands are the same and perturbations were largely the result of varying axial ligands or the nature of the R group of the (OOCR) bridges. The recent synthesis of dirhodium(II) complexes with hetero donor atoms in the basal plane, such as amidates²⁻⁷ or 2-hydroxypyridine⁸ provided systems with oxygen as well as nitrogen donors that are far more complex than the previous ones if for no other reason than the potential existence of geometrical isomers, even in the fully substituted derivative. The problem of multiple isomers is particularly acute when dealing with mixed systems (i.e., $x(\text{acetate}) + y(\text{amidate})$ ($x + y = 4$) produce a total of 12 theoretically isolable species), and it is this problem we are addressing in this study.

When hetero bridging ligands are employed, the environment in the equatorial planes is changed as a result not only of the presence of differences in ligands field strength but also of symmetry within the equatorial ligand field. For example, reference to Figure 1 demonstrates that, for the class of dinuclear complexes containing two acetates and two amidates, one can have one Rh with both nitrogens either in a cis or trans arrangement or one can have one nitrogen for each Rh ion; again, the arrangement can be cis or trans. The overall point group symmetry of these geometrical isomers are respectively C_s , C_2 , C_{2h} and C_1 . The effect of such changes on either local or overall point group symmetry is bound to reflect on the electronic structure of the rhodium dimer and on the Rh-Rh bond polarization, as well as on potential chemistry that may occur in the axial direction of a given metal component of the dimer. The first questions to be answered are as follows: Which of the possible isomers are produced in the

amidate-for-acetate exchange process? What are the factors involved in determining the observed isomer distribution? What are the chemical and structural consequences of amidate vs. carboxylate bridging? In this paper we present the answers to some of these questions.

Experimental Section

Chemicals. $\text{Rh}_2(\text{OOCCH}_3)_4$ was prepared from $\text{RhCl}_3 \cdot 3\text{H}_2\text{O}$ (Alfa Inorganics) by a literature method.⁹ Acetamide (Aldrich Chemical Co.) was recrystallized from benzene. All solvents used in this study were HPLC grade quality.

Preparation of $\text{Rh}_2(\text{OOCCH}_3)_x(\text{NHOCCH}_3)_{4-x}$. Two grams (4.52 × 10⁻³ mol) of $\text{Rh}_2(\text{OOCCH}_3)_4$ was mixed with 40 g (9.678 mol) of acetamide in a 250-mL round-bottom flask. The flask was evacuated and sealed by using a stopcock, placed in an oil bath at 125-135 °C, and magnetically stirred at this temperature for 24 h. During this period, the color of the molten mixture changed from green-blue to red-purple. After 24 h, the solution was cooled and the unreacted acetamide removed by sublimation. Another 40 g of fresh acetamide was added to the product, the flask evacuated, and the heating process continued for another 24 h. The excess acetamide was again removed by sublimation. The components of the product mixture were then separated by using HPLC.

Instrumentation. The chromatographic system consists of a Model 6000A solvent delivery system (Water Associates), an RCM-100 radial compression module containing a 10-cm Radial-PAK 10 μm CN column (Water Associates) and a Model 440 absorbance detector (Water Associates) operated at 254 nm (for analytical separations) and 546 nm (for semipreparative separations). The detector output was recorded on a Model 281 (Soltex) strip chart recorder. Isocratic methanol was used as the mobile phase in the HPLC separation. The separation was first carried out on an analytical scale by injecting 5 μL of an aqueous solution of the product mixture. At a flow rate of 4 mL/min, five well-separated bands were observed on the chromatogram. For the preparative scale separation, 500 μL of a concentrated aqueous solution of the mixture was injected at a flow rate of 4 mL/min. Under these conditions, five bands were observed and these were collected. The solvent was removed from each of the five samples collected and the complexes were dried in a vacuum oven at 100 °C for several hours. Elemental analyses of bands I-IV were performed by Galbraith Laboratories, Inc. and the results for the complex present in each of the LC bands is given below.

Anal. Calcd for band I, $\text{Rh}_2(\text{OOCCH}_3)_3(\text{HNOCCH}_3) \cdot \text{H}_2\text{O}$: C, 21.00; H, 3.27; N, 3.08. Found: C, 21.28; H, 3.27; N, 3.28.

Anal. Calcd for band II, $\text{Rh}_2(\text{OOCCH}_3)_2(\text{HNOCCH}_3)_2$: C, 21.81; H, 3.18; N, 6.36. Found: C, 21.62, H, 3.51, N, 6.28.

Anal. Calcd for band III, $\text{Rh}_2(\text{OOCCH}_3)(\text{HNOCCH}_3)_3$: C, 21.86; H, 3.41; N, 9.56. Found: C, 21.69; H, 3.83; N, 9.36.

(9) Rampel, G. A.; Legzdins, P.; Smith, H.; Wilkinson, G. *Inorg. Synth.* 1972, 13, 90.

- (1) Felthouse, T. R. *Prog. Inorg. Chem.* 1982, 29, 73 and references therein.
- (2) Dennis, A. M.; Howard, R. A.; Lancon, D.; Kadish, K. M.; Bear, J. L. *J. Chem. Soc., Chem. Commun.* 1982, 339.
- (3) Kadish, K. M.; Lancon, D.; Dennis, A. M.; Bear, J. L. *Inorg. Chem.* 1982, 21, 2987.
- (4) Duncan, J.; Malinski, T.; Zhu, T. P.; Hu, Z. S.; Kadish, K. M.; Bear, J. L. *J. Am. Chem. Soc.* 1982, 104, 5507.
- (5) Bear, J. L.; Zhu, T. P.; Malinski, T.; Dennis, A. M.; Kadish, K. M. *Inorg. Chem.* 1984, 23, 674.
- (6) Zhu, T. P.; Ahsan, M. Q.; Malinski, T.; Kadish, K. M.; Bear, J. L. *Inorg. Chem.* 1984, 23, 2.
- (7) Dennis, A. M.; Korp, J. D.; Bernal, I.; Howard, R. A.; Bear, J. L. *Inorg. Chem.* 1983, 22, 1522.
- (8) Cotton, F. A.; Felthouse, T. R. *Inorg. Chem.* 1981, 20, 584.

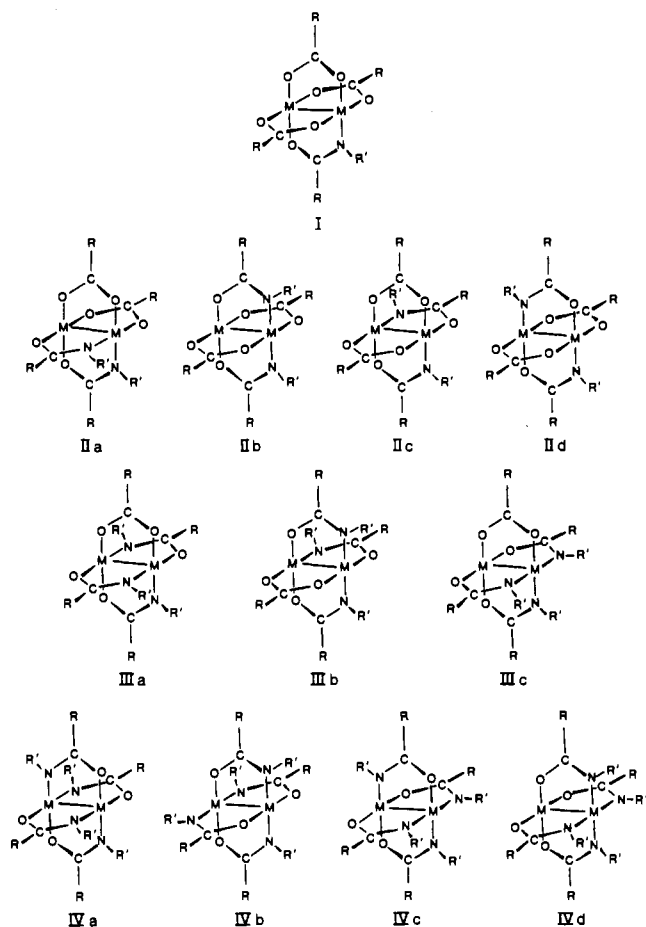


Figure 1. Structures of possible geometric isomers of the four substitution products. $\text{R} = \text{CH}_3$ and $\text{R}' = \text{H}$.

Anal. Calcd for band IV, $\text{Rh}_2(\text{HNOCCCH}_3)_4$: C, 21.91, H, 3.65; N, 12.78. Found: C, 21.85; H, 3.76; N, 12.33.

An experimental LC-MS instrument being developed by Vestal and co-workers¹⁰ (University of Houston) was used to determine the molecular mass of the complex (or complexes) in each of the LC bands. A 20- μL sample (in methanol) of the five LC bands collected was separately introduced into the mass spectrometer by means of a high-pressure loop injector and chromatographic pump. The methanol solution of the complexes entered the vaporizer through a stainless-steel capillary tube that was electrically heated to produce the thermal spray. The flow rate of the mobile phase was 0.5 mL/min. Using a soft ionization technique and operating in the negative or positive ion mode produced both negative and positive parent ions. The ions were observed by a quadrupole mass filter and electron multiplier with a 2000 amu range. The analog output was passed through an A/D converter into a Finnigan-INCOS 2300 data system.

The proton NMR spectra of the complexes were recorded with a Nicolet NT 300 spectrometer. All samples were dissolved in CD_3CN , and the chemical shifts were referred to Me_4Si as an internal standard. The XPS spectra of $\text{Rh}_2(\text{OOCCH}_3)_4$, $\text{Rh}_2(\text{OOCCH}_3)_3(\text{HNOCCCH}_3)$, $\text{Rh}_2(\text{OOCCH}_3)_2(\text{HNOCCCH}_3)_2$, $\text{Rh}_2(\text{OOCCH}_3)(\text{HNOCCCH}_3)_3$, and $\text{Rh}_2(\text{HNOCCCH}_3)_4$ were recorded on a PHI Model 550 spectrometer at an ambient temperature of 30 °C with monochromatized $\text{MgK}\alpha$ X-ray radiation. All complexes were dried at 90–100 °C under vacuum prior to preparation of sample for XPS measurements; 3–5 mg of the dried samples were then dissolved in hot acetonitrile. The solution was then placed dropwise on a pretreated, cleaned silver foil. As the solvent evaporated, a thin coat of the sample was obtained. At this time the color of the sample was red, indicating the acetonitrile adduct of the complexes. The sample was then placed in a vacuum dried and dried at 100 °C at 5–10 mmHg pressure for about 6 h. The color of the sample changed to blue/green, indicating no axially bound acetonitrile. A small amount of gold was deposited, by sublimation, on the surface of the sample in order to correct for any charging on the sample during the XPS measurement.

Table I. Binding Energies (eV) of Rhodium Complexes^a

compd	Rh 3d _{5/2}	C 1s ^b	O 1s	N 1s
$\text{Rh}_2(\text{OOCCH}_3)_4$	308.8	288.2	532.0	
$\text{Rh}_2(\text{OOCCH}_3)_3(\text{HNOCCCH}_3)$	308.6	287.8	531.5	398.6
$\text{Rh}_2(\text{OOCCH}_3)_2(\text{HNOCCCH}_3)_2$	308.4	287.4	531.4	398.4
$\text{Rh}_2(\text{OOCCH}_3)(\text{HNOCCCH}_3)_3$	308.2	287.0	531.4	398.2
$\text{Rh}_2(\text{HNOCCCH}_3)_4$	308.0	286.8	531.2	398.2
$\text{Rh}_2(\text{OOCCH}_3)_4^+$	310.3	288.3	532.2	
$\text{Rh}_2(\text{HNOCCCH}_3)_4^+$	308.9	286.8	531.2	398.2

^a Binding energy referenced to Au 4f_{7/2}. ^b Binding energy of carbonyl carbon.

Table II. Summary of Data Collection and Processing Parameters

space group	$C2/c$
cell const	$a = 11.466$ (1) Å $b = 12.290$ (3) Å $c = 14.812$ (4) Å $\beta = 96.83$ (1)°
temp	21 °C
cell volume	$V = 2072.42$ Å ³
axis of cryst alignment	[001]
mol formula	$[\text{C}_8\text{H}_{16}\text{N}_4\text{O}_4\text{Rh}_2 \cdot (2\text{H}_2\text{O})] \cdot 3\text{H}_2\text{O}$
M_r	528.128
density (calcd for $Z = 4$)	1.6925 g cm ⁻³
radiation	Mo K α ($\lambda = 0.71073$ Å)
abs coeff	$\mu = 14.75$ cm ⁻¹
data collcn range	4° < 2 θ < 55°
scan width	$\theta = (1.00 + 0.35 \tan \theta)$ °
max scan time	18 s
scan speed range	0.50–4.02° min ⁻¹
total no. of data colld	3967 ^a
no. of data with $I > 3\sigma(I)$	3233
total no. of variables	172
$R = \sum F_o - F_c / \sum F_o $	2.58%
$R_w = [\sum w^2(F_o - F_c)^2 / \sum w^2 F_o ^2]$	2.86%
minimized function	$\sum w(F_o - F_c)^2$
weights	$w = [\sigma(F_o)]^{-2}$
goodness of fit	2.20

^a Of these, 116 were standard and 618 were eliminated because they were weaker than the 3 σ criterion applied to the data.

Crystal Growth and X-ray Data Collection and Processing. The methanol solution of band IV from the HPLC separation was collected, and the solvent was evaporated on a rotary evaporator. The solid was dried in a vacuum oven at 100 °C overnight. The dried solid was dissolved in a minimum amount of distilled, deionized water, and the crystals were allowed to grow in a small vial by slow evaporation. After about 2 weeks, bright purple crystals were deposited at the bottom of vial.

The purple crystal selected for data collection was a nearly cubic specimen (since the dimensions of the sample were 0.20 × 0.18 × 0.17 mm and the transmission factors along these directions were calculated to be 0.7445, 0.7668, and 0.7782, no absorption correction was used), which was mounted in an arbitrary direction and oriented in a CAD-4 diffractometer equipped with a Mo target tube, with the radiation monochromatized by a dense graphite crystal. A set of 25 reflections, suitably spread over reciprocal space and with 2 θ ca. 30°, were used to define a primitive cell whose Niggli matrix¹¹ indicates the true cell is a C-centered monoclinic lattice. Tests for systematic absences showed the space group is either Cc or $C2/c$. Data collection (21 °C) produced 3233 independent data (see Table II), which were used for all subsequent calculations carried out with the SHELX-76¹² system of programs which employs the scattering curves of Cromer and Mann²⁵ for all atoms, except for hydrogens, which used the values of Stewart.²⁶ The Wilson plot and the distribution of unitary structure factors indicate the lattice is centrosymmetric, which, given the cell constants ($z = 4$), requires the molecules to lie at special positions.

A Patterson summation was computed that readily produced the location of the Rh atom. The first difference Fourier map computed produced most of the heavy atoms, the missing ones being found in the

(10) Blakley, C. R.; Carmody, J. J.; Vestal, M. L. *Anal. Chem.* **1980**, *52*, 1636.

(11) Niggli, R. "Handbuch für Experimentellphysik 7"; Akademische Verlagsgesellschaft: Leipzig, Germany, 1928; Teil 1, pp 108–176.
(12) Sheldrick, G. "SHELX-76 System of Computing Programs", Cambridge, England, 1976.
(13) Bear, J. L.; Kitchens, J.; Willcott, M. R. *J. Inorg. Nucl. Chem.* **1971**, *33*, 3479.

Table III. Positional Parameters with Estimated Standard Deviations

	x	y	z
Rh	0.54401 (2)	0.03784 (2)	0.07125 (1)
O1	0.6324 (2)	0.1081 (2)	0.2105 (1)
O2	0.3981 (2)	-0.0069 (2)	0.1324 (1)
O3	0.6165 (2)	-0.1135 (2)	0.1061 (1)
O4	0.5000 (0)	-0.2027 (2)	0.2500 (0)
O5	0.5000 (0)	0.2840 (3)	0.2500 (0)
O6	0.3576 (2)	-0.2625 (2)	0.1618 (2)
O7	0.2694 (2)	0.4152 (3)	0.1352 (2)
N1	0.6804 (2)	0.0761 (2)	0.0031 (2)
N2	0.4666 (2)	0.1781 (2)	0.0304 (2)
C1	0.3145 (2)	-0.0563 (2)	0.0819 (2)
C2	0.2103 (3)	-0.0922 (3)	0.1271 (3)
C3	0.5953 (2)	-0.1923 (2)	0.0482 (2)
C4	0.6436 (3)	-0.3014 (3)	0.0778 (3)
O1HA	0.625 (4)	0.069 (3)	0.255 (3)
O1HB	0.606 (3)	0.169 (3)	0.219 (3)
O4HA	0.465 (4)	-0.160 (3)	0.272 (3)
O5HA	0.551 (3)	0.319 (3)	0.284 (3)
O6HA	0.385 (4)	-0.306 (3)	0.186 (3)
O6HB	0.288 (4)	-0.366 (3)	0.188 (3)
O7HA	0.384 (4)	0.486 (3)	0.146 (3)
O7HB	0.307 (4)	0.415 (4)	0.135 (3)
N1H	0.726 (4)	0.110 (4)	0.021 (3)
N2H	0.477 (3)	0.236 (3)	0.055 (3)

Table IV. Bond Lengths (Å) and Angles (deg) and Their Estimated Standard Deviations

A. Bond Lengths			
Rh-Rh	2.415 (1)	C2-HA	0.87 (8)
Rh-O1	2.352 (2)	C2-HB	0.64 (9)
Rh-O2	2.069 (2)	C2-HC	0.91 (8)
Rh-O3	2.077 (2)	C4-HA	0.94 (4)
Rh-N1	2.015 (2)	C4-HB	0.69 (4)
Rh-N2	2.000 (2)	C4-HC	0.99 (4)
O1-H1	0.83 (4)	O4-HA	0.76 (4)
O2-H2	0.81 (4)	O5-HA	0.84 (4)
O2-C1	1.295 (3)	O6-HA	0.83 (4)
O3-C3	1.297 (3)	O6-HB	0.94 (4)
N1-C1	1.291 (3)	O7-HA	0.89 (4)
N2-C3	1.301 (3)	N1-H	0.69 (4)
C1-C2	1.503 (4)	N2-H	0.80 (4)
C3-C4	1.497 (4)		
B. Representative Hydrogen Distances			
O1-O6HB	1.88 (4)	O5-O1HB	1.96 (4)
O2-O1H2	1.95 (4)	O6-O7HA	1.91 (4)
O3-O7HA	2.20 (4)	O6-N1H	2.45 (4)
O3-O4HA	2.21 (5)	O7-O5HA	1.85 (4)
O4-O6HA	1.98 (4)	O7-C4HA	2.52 (4)
C. Bond Angles			
O1-Rh-O2	90.00 (1)	N1-Rh-Rh ¹	85.5 (1)
O1-Rh-O3	89.6 (1)	N2-Rh-Rh ¹	86.5 (1)
O1-Rh-N1	94.2 (1)	Rh-O2-C1	116.9 (2)
O2-Rh-N2	90.5 (1)	Rh-O3-C3	117.8 (2)
O3-Rh-N1	91.2 (2)	Rh-N1-C1	124.9 (2)
O3-Rh-N2	175.8 (1)	O2-C1-N1	122.4 (2)
N1-Rh-N2	87.8 (1)	O2-C1-C2	116.9 (3)
O1-Rh-N2	94.5 (1)	N1-C1-C2	120.6 (2)
O2-Rh-O3	88.5 (1)	O3-C3-C4	116.2 (2)
O1-Rh-Rh ¹	178.7 (1)	O3-C3-N2	122.0 (2)
O2-Rh-Rh ¹	90.3 (1)	N2-C3-C4	121.7 (3)
O3-Rh-Rh ¹	89.2 (2)		

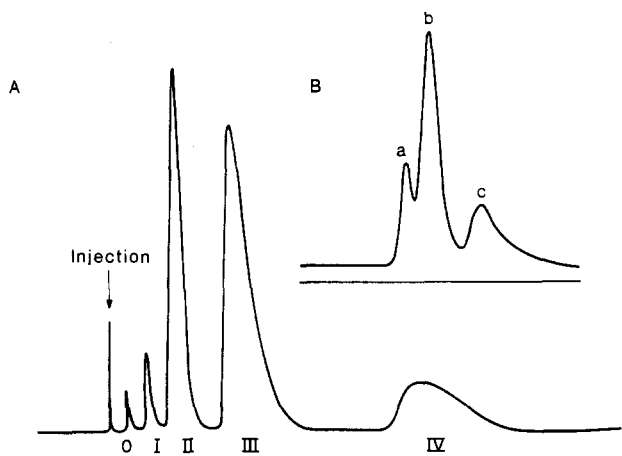


Figure 2. Chromatograms of the separation of (A) various substitution products at a flow rate of 4.5 mL/min and (B) separation of band II [$\text{Rh}_2(\text{OOCCH}_3)_2(\text{HNOCCCH}_3)_2$] at a flow rate of 0.5 mL/min.

next one. All the hydrogen atoms of the Rh molecule, as well as those of the waters of hydration were found experimentally and individually refined. The final positional parameters of the atoms are given in Table III. Details of all of the data collection parameters, data processing, and refinement information are listed in Table II. Table IV lists relevant bond lengths and angles, inter- and intramolecular bonds (including the axial waters) as well as hydrogen bonds for the three lattice waters. Tables of the equations of least-squares planes, the deviations of selected atoms therefrom, and dihedral angles are deposited as supplementary materials.

It is pertinent at this point to remark about the choice of oxygen vs. nitrogen in the acetamide ligands of this molecule: (a) the N-H hydrogen atoms that appear in the difference Fourier map clearly identify the nitrogen ligands; (b) the hydrogen atoms refine in their current location to a remarkably impressive stereochemical quality; (c) the overall refinement is excellent.

Results

High-Performance Liquid Chromatographic-Mass Spectrometry. The chromatogram presented in Figure 2 depicts the analytical scale separation of a 5- μL sample of the mixture of products obtained from the reaction of $\text{Rh}_2(\text{OOCCH}_3)_4$ with molten acetamide. The parent ion masses of the isomeric mixtures present in the five bands corresponded to those of composition $\text{Rh}_2(\text{OOCCH}_3)_4$, $\text{Rh}_2(\text{OOCCH}_3)_3(\text{HNOCCCH}_3)$, $\text{Rh}_2(\text{OOCCH}_3)_2(\text{HNOCCCH}_3)_2$, $\text{Rh}_2(\text{OOCCH}_3)(\text{HNOCCCH}_3)_3$, and $\text{Rh}_2(\text{HNOCCCH}_3)_4$, respectively for bands 0-IV. When each band was subjected to HPLC at a much slower solvent flow rate (0.5 mL/min), band

II split into three overlapping components. Since all three of the components have a parent mass peak of 440 amu, they must be three of the four geometric isomers (IIa-d, Figure 1) possible for this 2:2 composition. The other bands did not split at the slower flow rate but neither band 0 nor band I is expected to do so since these bands are the parent tetraacetate and the only species with three acetates and one acetamide (Figure 1, I). However, bands III and IV could, in theory, consist of as many as seven isomers. The negative results may merely mean that the LC method used is incapable of effecting the separation—a strange result, if correct, given the wide difference in polarity of some of those isomers. Furthermore, crystallization of the contents of band III produces a single, chemically and crystallographically well-behaved species whose molecular formula is $\text{Rh}_2(\text{OOCCH}_3)(\text{HNOCCCH}_3)_3$, and its structure¹⁴ corresponds to IIIa of Figure 1. Likewise, band IV produces exclusively isomer IVa (Figure 1) of $\text{Rh}_2(\text{HNOCCCH}_3)_4$ as shown by NMR and crystallography (see crystallographic details below). Therefore, it would appear that the only substitution product that is formed as a mixture of geometric isomers is the 2:2 acetate:acetamide derivative.

Nuclear Magnetic Resonance. The complex in LC band I, $\text{Rh}_2(\text{HNOCCCH}_3)(\text{OOCCH}_3)_3$ displays three NMR peaks at 1.76, 1.6, and 1.87 ppm with an area ratio of 2:1:1. For this complex the two acetates trans to each other have magnetically equivalent methyl groups, and the amide methyl and trans acetate methyl are different. The problem with the product found in LC band II is that it is a mixture of at least three geometric isomers of $\text{Rh}_2(\text{HNOCCCH}_3)_2(\text{OOCCH}_3)_2$. Each of the geometric isomers of the disubstituted complex $\text{Rh}_2(\text{OOCCH}_3)_2(\text{HNOCCCH}_3)_2$ should display two methyl proton peaks. Therefore, a mixture of three geometric isomers could show six proton resonances, and these are observed at 2.15, 1.84, 1.74, 1.73, 1.72, and 1.64 ppm. The complex in LC band III gives four peaks at 1.78, 1.77, 1.68, and 1.67 ppm with area ratios of 1:1:1:1. The only isomer of

(14) Ahsan, M. Q.; Bernal, I.; Bear, J. L., unpublished data.

$\text{Rh}_2(\text{HNOCCH}_3)_3(\text{OOCCH}_3)$ that would give this NMR spectrum is the one with two cis nitrogens on one rhodium and one nitrogen on the other. The molecular structure of $\text{Rh}_2(\text{HNOCCH}_3)_4$, which is found in LC band IV, is reported in this paper. This complex has two cis nitrogens on each rhodium; thus, the NMR spectrum shows one resonance for the protons of all four methyl groups at 2.20 ppm since they are magnetically equivalent.

X-ray Photoelectron Spectra. The X-ray photoelectron spectra of the mixed substitution products, $\text{Rh}_2(\text{HNOCCH}_3)_4$, and $\text{Rh}_2(\text{HNOCCH}_3)_4^+$ were recorded in this study, and the binding energies for the rhodium $3d_{5/2}$ electrons are listed in Table I. Also listed in the table are binding energies of $\text{Rh}_2(\text{OOCCH}_3)_4$ and $\text{Rh}_2(\text{OOCCH}_3)_4^+$. All of the complexes show a single Rh $3d_{5/2}$ peak, implying that within the sensitivity of the XPS measurement identical rhodium ions exist in each dimeric complex. The binding energy of Rh $3d_{5/2}$ decreases by 0.2 eV for each acetamidate substitution and it is interesting to note that removal of an electron from $\text{Rh}_2(\text{HNOCCH}_3)_4$ to form $\text{Rh}_2(\text{HNOCCH}_3)_4^+$ causes a increase in the $3d_{5/2}$ binding energy of 0.90 eV, resulting in a binding energy for $\text{Rh}_2(\text{HNOCCH}_3)_4^+$ approximately equal to that for $\text{Rh}_2(\text{OOCCH}_3)_4$.

Discussion of Chemistry and Spectral Data

There are numerous examples in the literature involving the synthesis of dinuclear rhodium (II) complexes by the exchange of bridging ligands.¹ However, there is surprisingly little information concerning the mechanism of the exchange process. Several years ago, we reported the results of a kinetic study involving the reaction of dirhodium(II) tetraacetate with trifluoroacetic acid.¹³ The measured rate constants for the stepwise exchange of trifluoroacetate for acetate were found to have a ratio of 1:2:0.1:0.025 for $k_1:k_2:k_3:k_4$. The first trifluoroacetate substitution has a labilizing influence on the complex, causing the second substitution to occur approximately twice as fast. The third and fourth exchange reactions do not show this labilizing effect and, in fact, show the complex to be rather kinetically inert after the formation of the disubstituted complex. From these results we were able to conclude that the substitution reaction proceeds in a stepwise manner and the addition of each trifluoroacetate bridge alters the rate of the subsequent exchange in a way not predicted from purely statistical considerations.

The exchange reaction involving $\text{Rh}_2(\text{OOCCH}_3)_4$ and acetamide is different since acetamide is a much weaker acid than any carboxylic acid and the acetamidate ion is a better σ -donor and worse π -acceptor of electron density. Also, with this hetero donor bridging ion the sequence and geometric location of bond breaking and bond formation process are reflected in the final products in the form of geometric isomers of the di-, tri-, and tetraamidate complexes.

There are 14 possible products from the reaction of $\text{Rh}_2(\text{OOCCH}_3)_4$ with acetamide (Figure 1) since IIId and IIIa also have optical isomers. If the substitution of each acetamidate ion has a directing influence on the location (cis or trans) and bonding orientation (N or O) of the subsequent acetamidate exchange and the acetamidate ion only substitutes for acetate ions, then the number of isomers produced for each substitution product should be small. However, if the directing influences are weak a large number of isomers could be formed.

The results derived from the analytical scale separation and mass spectra of the separated bands show that three isomers of group II, one isomer of group III, and one isomer of group IV are formed. The molecular structure of the tetrasubstituted complex, $\text{Rh}_2(\text{HNOCCH}_3)_4$, is reported in this paper and reveals the complex to be isomer IVa. The molecular structure of the trisubstituted complex $\text{Rh}_2(\text{HNOCCH}_3)_3(\text{OOCCH}_3)-2(\text{CH}_3)_2\text{SO}$ has also been determined, and the results show the complex to be isomer IIIa.¹⁴ The proton NMR spectrum of the trisubstituted complex is also consistent with isomer IIIa, which has four magnetically nonequivalent methyl groups. It might also be pointed out that IIIa is the only trisubstituted isomer that can produce IVa if only acetamidate for acetate exchange is occurring. Among the four isomers of $\text{Rh}_2(\text{HNOCCH}_3)_2(\text{OOCCH}_3)_2$ only

isomer IIb is incapable of forming IIIa. Therefore, the three isomers of the disubstituted complex produced in the reaction appear to be IIa, IIc, and IIId. The LC peak areas show that one of the isomers is produced in considerable excess over the other two. Unfortunately, we have not been able to separate and collect these isomers in sufficient amounts for structure determination.

The selectivity of the reaction to produce only one isomer of the tri- and tetraamidate-substituted complexes suggest that only acetamidate for acetate exchange occurs and that the addition of each acetamidate bridge has a directing influence on the next substitution. The fact that no isomer is produced with two nitrogens trans to each other on the same rhodium ion shows that the directing influence of an acetamidate bridge involves both the location and bonding orientation of the entering amidate ion. In fact the only restriction that needs to be placed on the exchange processes is that the nitrogen of the entering amidate ion cannot bind trans to any other nitrogen on the same rhodium ion. With this restriction, the observed and predicted isomer distribution are the same. Cotton et al. isolated three products from the reaction of $\text{Rh}_2(\text{OOCCH}_3)_4$ with 2-methyl-6-hydroxypyridine.⁸ In contrast to our results, all three complexes had two trans nitrogens on one or both the rhodium ions, and none of the isomers we found for the acetamide systems were isolated by them. We have also found that when *N*-phenylacetamide is used as the substituting ligand two tetra-substituted isomers are produced in significant amounts,⁴ one of these isomers has three nitrogens on one rhodium and one on the other. Therefore, it is obvious that the nature of the hetero donor atom ligand plays a major role in determining the isomer distribution in the substitution products. The two most obvious factors involved in determining the orientation and equatorial position of an entering acetamide ion are the nature of the axial bond prior to equatorial substitution (Rh-N vs. Rh-O) and the directing influence of equatorially bound amidate ions. A more detailed study is required to determine the relative importance of these factors. For example, in the case of 2-methyl-6-hydroxypyridine the negative charge resides primarily on the oxygen, after deprotonation, and axial bonding has to occur through the oxygen because of steric constraints on the pyridyl nitrogen. Also the pyridyl nitrogen is not nearly as basic as the acetamidate nitrogen and would produce a different electronic effect in the position trans to the Rh-N equatorial bond.

The next question to be addressed is how the chemical reactivity at the axial position is affected by acetamidate for acetate exchange. In a recent publication⁶ it was reported that the first oxidation potential of the dirhodium(II) complex is lowered ~ 0.25 V by the addition of each acetamidate bridge, resulting in a lowering of 1.0 V for the totally substituted complex. This could result from the energy of the HOMO being selectively sensitive to the symmetry and strength of the acetamidate ligand field or a uniform increase in the energy of the metal-centered orbitals due to charging by the less electronegative acetamidate bridging ions. The XPS data shown in Table I supports the latter. The binding energy of the Rh $3d_{5/2}$ of the acetamidate complexes is affected to almost the same degree as the energy of the HOMO. An interesting comparison can be made from the Rh $3d_{5/2}$ binding energies of $\text{Rh}_2(\text{OOCCH}_3)_4$, $\text{Rh}_2(\text{HNOCCH}_3)_4$ and $\text{Rh}_2(\text{HNOCCH}_3)_4^+$. The addition of each acetamidate bridge decreases the binding energy by ~ 0.25 eV, resulting in a change from 308.8 eV for $\text{Rh}_2(\text{OOCCH}_3)_4$ to 308.0 eV for $\text{Rh}_2(\text{HNOCCH}_3)_4$. The binding energy of the radical cation $\text{Rh}_2(\text{HNOCCH}_3)_4^+$ is 308.9 eV, which is about the same within experimental error (± 0.1 eV) as that of $\text{Rh}_2(\text{OOCCH}_3)_4$. Therefore, the substitution of four acetamidate ions for acetates results in an increase in electron density on the dirhodium(II) centers equivalent to the addition of one electron. In fact, the Rh $3d_{5/2}$ binding energy for $\text{Rh}_2(\text{HNOCCH}_3)_4$ is even less than that observed for the rhodium(I) complex $\text{Rh}(\text{PPh}_3)_3\text{Cl}$.¹⁵ These results suggest that the $\text{Rh}_2(\text{HNOCCH}_3)_4$ should be a much better π -donor and weaker σ -acceptor than $\text{Rh}_2(\text{OOCCH}_3)_4$ with respect to axial bonding. In order to investigate this possibility, as well as to determine which geometric isomer was produced in the exchange reaction, we recently determined the crystal and mo-

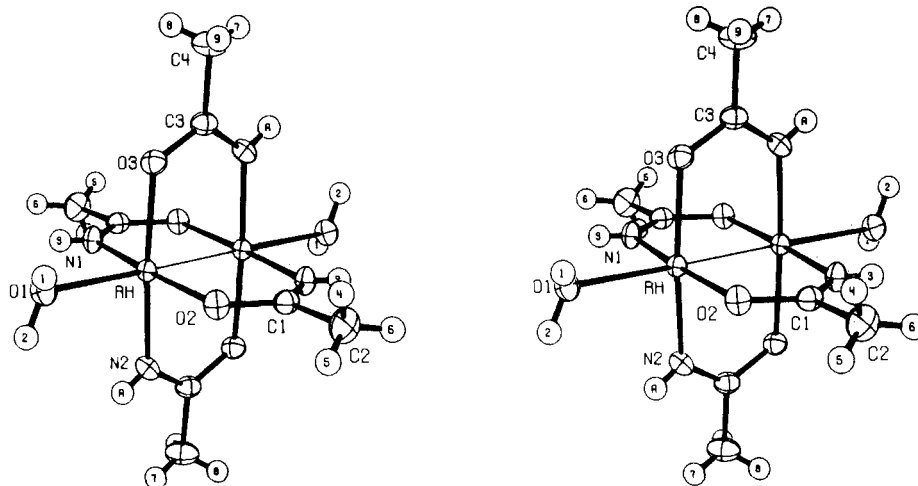


Figure 3. Molecular structure of $[\text{Rh}_2(\text{HNOCCH}_3)_4 \cdot 2\text{H}_2\text{O}] \cdot 3\text{H}_2\text{O}$. This is a stereopair.

molecular structure of $[\text{Rh}_2(\text{OOCCH}_3)(\text{HNOCCH}_3)_3 \cdot 2(\text{CH}_3)_2\text{S-O}] \cdot 2\text{H}_2\text{O}$ ¹⁴. Even though $(\text{CH}_3)_2\text{SO}$ is not the strongest π -acceptor ligand available, we assumed that if there is a significant π -interaction between the filled Rh_2 π orbitals and the empty orbitals of S, a shorter Rh-S distance would be observed than that reported for $[\text{Rh}_2(\text{OOCCH}_3)_4((\text{CH}_3)_2\text{SO})_2]$. We found that this is the case.¹⁴ The Rh-S bond for the triacetamidate complex is 0.038 Å shorter than that of the corresponding tetraacetate complex.¹⁶ This is particularly significant when we consider that the Rh-OH₂ bond for the tetraacetamidate complex reported in this paper is 0.042 Å longer than the Rh-OH₂ bond reported for the tetraacetate adduct.¹⁵

Stereochemical Discussion

A. Stereochemistry of the Complexes and Packing Information.

As can be seen in Figures 3 and 4 (Figure 4 is supplemental material) geometrical isomer IVa has the classic features of bimetallic species of composition $\text{M}_2(\text{bridging ligand})_4\text{L}_2$ ($\text{M} = \text{Cr}, \text{Mo}, \text{Cu}, \text{Rh}, \text{Ru}, \text{etc.}$) ours being only the second example of the use of the asymmetric acetamide ligand. The previous example, $\text{Rh}_2(\text{HNOCCF}_3)_4 \cdot 2\text{C}_2\text{H}_5\text{N}$, was structurally characterized here also but was not of the quality of the present study due to lattice disorder problems.⁷ However, the current results indicate that all arguments used in the previous study concerning the nature of the geometric isomer, and the identification of N vs. O were correct, as we shall see below.

Since the hydrogen atoms in the molecular diagram (Figure 3) are shown at their refined values, it is clear that in this case there is no ambiguity concerning the nature of the binding site (N vs. O); furthermore, reversal of the scattering curves for those two atoms makes the thermal parameters larger for the "O" and smaller for the "N", indicating that reversal is incorrect. In any case, the presence of refined hydrogen atoms is sufficient proof of our correct choice but we wanted to point out the consistency of these two results. Finally, the following items of consistency are remarked upon at this point. Note (Figure 3) that a nonbonded pair lobe of the axial water is directed to the N-H hydrogen—an eminently sensible thing to do since, were this an amido oxygen, there would be two nonbonded oxygen lone pairs pointing at each other. One also notes that the shortest hydrogen bonded contact is between O1 and H6B (a water hydrogen; 1.88 Å) whereas the shortest contact on the other side is between the H of NH and O6 (2.45 Å). Again, the consistency is satisfying since one can use this lattice-water argument in the future with lesser quality structures in which the hydrogen atoms cannot be identified directly.

B. Bonding within the $\text{Rh}_2(\text{HNOCCH}_3)_4 \cdot 2\text{H}_2\text{O}$ Molecules. First we will compare internally our results for IVa and note that the two independent Rh-N distances are 2.015 (2) and 2.000 (2) Å

(average 2.008 (2) Å) while the Rh-O distances are 2.069 (2) and 2.077 (3) Å (average 2.073 (2) Å). That is, the former are clearly shorter than the latter. The same situation was observed for $\text{Rh}_2(\text{HNOCCF}_3)_4 \cdot 2\text{py}$, the Rh-N distances were 2.01 (1) and 1.98 (1) Å while the Rh-O distance was 2.12 Å. However, in the case of the substituted 2-hydroxypyridine complexes reported by Cotton et al.,⁸ there is considerable variation among the Rh-N and Rh-O bond distances but in all cases the Rh-N distance is longer than the Rh-O distance. These results strongly suggest that the strength of the Rh-donor atom bond in the basal plane is a function of the basicity of the donor atom. There is, therefore, a lengthening of the Rh-O bonds in IVa, which is, no doubt, due to a trans effect caused by the stronger covalent bonding ability of the amide N donors opposite the oxygens of the basal plane. This trans effect is most certainly a factor in determining the isomer distribution observed for the products of the acetamidate for acetate exchange reaction. An interesting feature of IVa is the large difference in the Rh-O-C (average 117.4°) and Rh-N-C (average 124.9°) angles of the bridging acetamidate ion. Also the two oxygens are very close to the equatorial plane (average Rh-Rh-O = 89.8°) whereas the acetamidate nitrogens lie out of the plane displaced toward the second rhodium ion (average Rh-Rh-N = 86°). Since there are no steric reasons for this molecular distortion, it must be due to electronic effects in this orbitally complex system. Another interesting point concerning the basal plane bonds is this: if an axial ligand has perfect cylindrical symmetry, as in the case of CO or CN, for example, one would expect that the basal plane bonds would be identical within experimental error. However, this is seldom the case since most of the axial ligands are asymmetric with respect to that plane. For example, water has a pair of asymmetrically directed nonbonded pairs on one side and two hydrogens on the other. In our case (IVa) we can see (Figure 3) that one of the axial water's nonbonded pairs selects N1-H to point to. The same argument can be made with most compounds of this class since nonbonded pairs, atoms, groups, π -bonds, etc.... are trapped into specific orientations in the solid state and seem to influence the bonding in the basal plane.¹⁶⁻¹⁸ A few examples are

compd	Rh-N, Å	Rh-O, Å	ref
$\text{Rh}_2(\text{HNOCCH}_3)_4 \cdot 2\text{H}_2\text{O}$ (IVa)	2.015, 2.000	2.069, 2.077	here
$\text{Rh}_2(\text{OOCCH}_3)_4 \cdot 2\text{H}_2\text{O}$ (V)		2.029, 2.042	17
		2.036, 2.047	
$\text{Rh}_2(\text{OOCCH}_3)_4 \cdot 2(\text{CH}_3)_2\text{SO}$ (VI)		2.029, 2.038	16
$\text{Rh}_2(\text{OOCCH}_3)_4 \cdot 2\text{C}_2\text{H}_5\text{N}$ (VII)		2.035, 2.042	18
$\text{Rh}_2(\text{OOCMe}_3)_4 \cdot 2\text{H}_2\text{O}$		2.036, 2.045	18

(16) Cotton, F. A.; Felthouse, T. R. *Inorg. Chem.* **1980**, *19*, 323.

(17) Cotton, F. A.; DeBoer, B. G.; LaPrade, J. R.; Ucko, D. A. *Acta Crystallogr., Sect. B: Struct. Crystallogr. Cryst. Chem.* **1971**, *B27*, 1664.

(18) Koh, Y. B.; Christoph, G. G. *Inorg. Chem.* **1978**, *17*, 2590.

(15) Imanaka, T.; Kaneda, K.; Teramishi, S.; Terasawa, M. *Proc. Int. Congr. Catal.*, 6th. 1977, *2*, 509.

For all of these compounds, the apparently high symmetry of the basal plane is broken in the solid by specific arrangements of asymmetry-inducing portions of the axial ligands, introducing small but measurable differences in the bonds at the base. Reference to the recent review by Boyar and Robinson¹⁹ reveals that this is, indeed, a general trend for all these substances, which is most readily noted in the more accurate structural determinations.

We now turn our attention to the amide ligand and note that there is a marked change in the C–N bond upon ionization and complexation. Bernal and Korp²⁰ determined the structure of a free benzamide of composition $(\text{Ph})-\text{C}(=\text{NR})(\text{NHR})$, with $\text{R} = \text{CH}(\text{Me})\text{Ph}$, $\text{Me} = \text{methyl}$, $\text{Ph} = \text{phenyl}$. In this substance, the single- and double-bonded amidine nitrogens have C–N bond lengths of 1.36 (1) and 1.28 (1) Å. In Va, the average C–N length is 1.296 Å—a value closer to that for a pure C=N double bond (1.255 Å²³) than that for a single C–N bond associated with an sp^2 -hybridized C atom (1.45 Å²⁴).

Next we consider the axial bonds in IVa. The most reasonable model to compare this molecule with is the tetraacetate dihydrate (hereafter V) since we can evaluate the effect of changing NH for O in the basal plane on the axial Rh–Rh and Rh–OH₂ bonds. For example, Cotton, et al¹⁷ reported an axial Rh–O distance of 2.310 (3) Å whereas in Va this distance is 2.353 (2) Å; the difference ($\Delta = 0.043$ Å) is meaningful to the extent of ca. 12σ . Parallel with this lengthening of the Rh–O distance, one notes that the Rh–Rh distance in V and IVa are, respectively, 2.386 (5) and 2.415 (1) Å. Again, there is a destabilizing effect on this axial bond due to the introduction of the two NH groups. One is tempted to explain the increase in both the Rh–axial ligand and Rh–Rh bond length for IVa by the increased electron density on the rhodium centers brought about by the acetamidate bridges. However, a different result is observed for changes in metal-centered electron density resulting from the substitution of CH_3 by CF_3 in the tetraacetate complex.²¹ As expected, the Rh–axial ligand bond length decreases; however, the Rh–Rh distance as well as the O–C–Y (Y = O or NH) bond angle increase. It appears that for carboxylates there is a predictable relationship between the Rh–Rh and Rh–axial ligand bond length and the electron-donor properties of the bridging ligand. However, the relationship is not as clear when carboxylates are compared with the corresponding amidates. This is not unexpected since the dirhodium(II) tetraamidates appear to be much better π -donors and weaker σ -acceptors with respect to axial bonding.²²

Another factor which is not understood is the following: To what extent is the preferred O–C–Y angle of the bridging ligand involved in determining the Rh–Rh bond distance? It appears that the carbonyl substituents, R and Y of $\text{RC}(\text{O})\text{Y}$, have a much greater effect on the O–C–Y angle than any other factor. For example the bridging angle for IV is 2.6° less than that reported for V even though the Rh–Rh bond length is greater for IVa. Also, as stated earlier, the substitution of CF_3 for CH_3 in both IVa⁷ and V²¹ increases the bridging angle by $\sim 5^\circ$.

C. The Packing of the Waters of Hydration. As can be appreciated from the the packing diagram (Figure 4, supplementary material) and from the nature of the position of the oxygen (H_2O) atoms (see Table III) the three waters of hydration are so distributed in the lattice that two are in general positions (O6 and O7) while two half-waters (O4 and O5) lie on mirror planes. The mirrors bisect those waters for which there is only one independent hydrogen per oxygen atom. In the packing diagram, those waters are at the extremes of the hexagonal ring appearing on the lower right and upper left corners of the cell. Looking at the ring of waters on the upper part of the cell, we note that the rightmost water points both its hydrogens to adjacent waters; the next two waters, on either side of the ring, use only one hydrogen atoms to bond to the subsequent waters. Finally, the sixth one (and last member of the ring) is the only one with an oxygen surrounded by four hydrogens (its own two plus two more from hydrogen bonds). This last water is the only one behaving as do the water molecules of ice II, which, in both its hexagonal and cubic forms, consists of six-membered rings, all of whose waters contain as a building block the tetrahedral H_4O moiety. However, in those cases, the rings are not planar but rather resemble cyclohexane. Our ring is nearly planar (see Table V, supplementary material with maximum deviations from the mean plane of oxygens of 0.18 Å (see Table V, supplementary material).

Acknowledgment. We thank the Robert A. Welch Foundation (J.L.B. and M.Q.A., Grant E-918; I.B., Grant E-594) for support of this work.

Registry No. 1, 99631-49-9; $\text{Rh}_2(\text{OOCCH}_3)_3(\text{HNOCCH}_3)$, 87985-37-3; $\text{Rh}_2(\text{OOCCH}_3)_2(\text{HNOCCH}_3)_2$, 87985-38-4; $\text{Rh}_2(\text{OOCCH}_3)(\text{HNOCCH}_3)_3$, 87985-39-5; $\text{Rh}_2(\text{HNOCCH}_3)_4$, 87985-40-8; $\text{Rh}(\text{OOCCH}_3)_4^+$, 83681-59-8; $\text{Rh}(\text{HNOCCH}_3)_4^+$, 87985-44-2; Rh, 7440-16-6.

Supplementary Material Available: A molecular packing diagram and tables containing observed and calculated structure factors, thermal parameters, and least-squares planes, related dihedral angles, and deviations of selected atoms (Table V) (22 pages). Ordering information is given on any current masthead page.

(19) Boyar, B.; Robinson, Stephen D. *Coord. Chem. Rev.* **1983**, *50*, 109–208.

(20) Korp, J. D.; Bernal, I. *Chem. Scr.* **1983**, *20*, 60–63.

(21) Cotton, F. A.; Felthouse, T. R. *Inorg. Chem.* **1982**, *21*, 2667.

(22) Chavan, M. Y.; Zhu, T. P.; Lin, X. Q.; Ahsan, M. Q.; Bear, J. L.; Kadish, K. M. *Inorg. Chem.* **1984**, *23*, 4538.

(23) Nardelli, M.; Fava, G. *Acta Crystallogr.* **1962**, *15*, 214.

(24) Pauling, L. "The Nature of the Chemical Bond", 3rd ed.; Cornell University Press: Ithaca, NY, 1960.

(25) Cromer, D. T.; Mann, J. B. *Acta Crystallogr., Sect. A: Cryst., Phys., Diffr. Theor. Gen. Crystallogr.* **1968**, *A24*, 321.

(26) Stewart, R. F.; Davidson, E. R.; Simpson, W. T. *J. Chem. Phys.* **1965**, *42*, 3175.